A demonstration of donor passivation through direct formation of V-As-i complexes in As-doped $Ge_{1-X}Sn_x$

A demonstration of donor passivation through direct formation of V-As$_i$ complexes in As doped Ge$_{1-x}$Sn$_x$

Afrina Khanam,[1,2,*] Anurag Vohra,[3,4] Jonatan Slotte,[1,2] Ilja Makkonen,[2,5]

Roger Loo,[4] Geoffrey Pourtois,[4,6] and Wilfried Vandervorst[3,4]

[1]*Department of Applied Physics, Aalto University,*

P.O. Box 15100, FI-00076 Aalto, Finland

[2]*Department of Physics, P.O. Box 43,*

FI-00014 University of Helsinki, Finland

[3]*K.U. Leuven, Department of Physics and Astronomy,*

Celestijenlaan 200D, 3001 Leuven, Belgium

[4]*Imec vzw, Kapeldreef 75, 3001 Leuven, Belgium*

[5]*Helsinki Institute of Physics, P.O. Box 43,*

FI-00014 University of Helsinki, Finland

[6]*Department of Chemistry, Plasmant Research Group,*

University of Antwerp, B-2610 Wilrijk-Antwerp, Belgium

Abstract

Positron annihilation spectroscopy in Doppler and coincidence Doppler mode was applied on Ge$_{1-x}$Sn$_x$ epitaxial layers, grown by chemical vapor deposition with different total As concentrations ($\sim 10^{19} - 10^{21}$ cm^{-3}), high active As concentrations ($\sim 10^{19}$ cm^{-3}), and similar Sn concentrations ($5.9 - 6.4\%$). Positron traps are identified as mono-vacancy complexes. Vacancy-As complexes, V-As$_i$, formed during the growth were studied to deepen the understanding of the electrical passivation of the Ge$_{1-x}$Sn$_x$:As epilayers. Larger mono-vacancy complexes, V-As$_i$ ($i \geq 2$) are formed as the As doping increases. The total As concentration shows a significant impact on the saturation of the number of As atoms ($i = 4$) around the vacancies in the sample epilayers. The presence of V-As$_i$ complexes decrease the dopant activation in the Ge$_{1-x}$Sn$_x$:As epilayers. Furthermore, the presence of Sn failed to hinder the formation of larger V-As$_i$ complexes and thus failed to reduce the donor-deactivation.

---

[*] Email:afrina.khanam@aalto.fi

I. INTRODUCTION

Si achieved priority over Ge in device fabrication owing to its larger band gap, a low surface-state density and a stable oxide. [1] However, transistors built out of pure Ge can attain three times higher electron and four times higher hole mobilities due to the low effective masses of the charge carriers compared to those of Si at low electric fields. [2] This has led to revive the implementation of Ge in the miniaturization of field effect transistors (FET), building mid-infrared photodetectors, and designing both logic and photonic device applications. [3–6] Transistor scaling requires an increase in the concentration of electrically active donor and acceptor atoms to maintain a constant total charge in the source and drain region. [7] $Ge_{1-x}Sn_x$ epilayers grown on Si substrates are playing an interesting role in logic applications for strain engineering and in photonics due to its optical gain. [5, 8] $Ge_{1-x}Sn_x$ channel pMOSFETs have been shown to achieve higher hole mobility than Ge channel pMOSFETs. [9] Epitaxial $Ge_{1-x}Sn_x$ films mixed with Si are suitable for the source-drain (S/D) stressors of the n-FETs to maintain sufficient conductivity of the channel between the source and the drain. Milazzo $et\ al.$ suggested that Excimer Laser Annealing (ELA) can be used to activate implanted Arsenic (As) in Ge to form n-type Ultra-shallow junctions (USJs) with a high active doping concentration of $\sim 10^{20}$ cm^{-3}. [10]

Point defects and defect complexes in semiconductors can introduce energy levels in the forbidden band gap that act as compensating centers and charge carrier traps. The intricate electrical and structural properties of defects and defect complexes in Ge have been analysed by means of Deep Level Transient Spectroscopy (DLTS). [11] Either P, As, Sb or Bi doped n-type oxygen lean Ge crystals with doping concentrations of $10^{13} - 10^{15}$ cm^{-3} were studied by Markevich $et\ al.$ by means of the capacitance-voltage, the current-voltage techniques and DLTS. [12] They showed that E-centers have three charge states in the band gap: double negative, single negative, and neutral. Nylandsted Larsen and Mesli reported on a third transition level in Sb doped irradiated Ge, where the $(+/0)$- and $(0/-)$-states are located below mid gap and the $(-/--)$-state is in the upper half of the band gap at $E_c - 0.30$ eV. [11] A detailed DLTS investigation of radiation damage introduced in p-type Ge by high energy electrons, protons, and alpha particles had been carried out by Petersen $et\ al.$ to study divacancy defects. They identified one acceptor level associated with the divacancy at $E_v + 0.19$ eV which likely accounted for both a single and a double acceptor level due to an

inverted ordering of the levels. [13] In a study of intrinsic and extrinsic diffusion of n-type dopants in Ge, Brotzmann *et al.* showed that the simultaneous diffusion of n-type dopants and self-atoms is caused by the presence of doubly negatively charged vacancies (V^{2-}). [14] They also suggested that the diffusion of all n-type dopants *e.g.* P, As, and Sb exceeds Ge self diffusion which reveals an attractive interaction between the dopants and the vacancies leading to the formation of dopant-vacancy pairs. [14] They concluded that the activation enthalpy of dopant diffusion for intrinsic conditions decreases with increasing size of the n-type dopants. This indicates an increasing binding energy between the dopant and the vacancy. [14] Brotzmann *et al.* reported on the stabilization of donor-vacancy complexes in Ge and the dopant deactivation via the formation of dopant-vacancy complexes in a research on diffusion of self-atoms and n-type dopants in Ge studied by means of controlled multilayer structures. [15]

The Positron Annihilation Spectroscopy (PAS) technique is well suited to analyse open volume point defects in solids. [16, 17] Annealing behaviour in electron irradiated Ge was analysed with PAS by Polity *et al.* [18] The identification of mono- and divacancies with PAS in Ge presents an example for narrow band gap semiconductors. [19, 20] The existence of Ge mono-vacancy at the temperature of 100 K, along with the observation of mobile mono-vacancies pairing up to form divacancies at 200 K was reported by Slotte *et al.* [19] Kuitunen *et al.* observed clustering of divacancies at elevated temperatures in neutron-irradiated n-type Ge. [20] Additionally, Slotte *et al.* showed a free volume of divacancy size in as-implanted Ge applying PAS. [21] Recently, Kujala *et al.* [22] and Kalliovaara *et al.* [23] applied the PAS technique to study vacancies and vacancy clusters in P, As, and Sb doped Ge, and in highly As doped Ge, respectively. Using Czochralski-grown bulk Ge in which diffusion anneals with As was performed at 680 °C, Kujala *et al.* showed that, the dopant complex accounting for positron trapping is a vacancy multi-donor defect complex with three As atoms around the vacancy. [22] In the study of highly As-doped Ge, where samples were implanted with 40 keV As^+ ions, subjected to ELA and recrystallized, a high concentration of vacancy-As complexes larger in open volume than a mono-vacancy was observed by Kalliovaara *et al.* [23] Their studies revealed that, divacancy complexes contribute substantially to the large inactive fraction of the donors in As-implanted laser annealed Ge. In a previous study, we showed that mono-vacancy size defects are surrounded by one to at least three P atoms depending on the P-doping level in epitaxial Ge applying

PAS. [24] In a separate study, we focused on the defect analysis on $Ge_{1-x}Sn_x$ epilayers doped with P utilizing PAS. [25] The study revealed that, the strong interaction of vacancies with the P atoms is the reason behind the dominant dopant deactivation in $Ge_{1-x}Sn_x$:P. [25]

In this work, we applied PAS to As doped $Ge_{1-x}Sn_x$ epilayers to analyse the vacancy-donor complexes. Since compensation of dopants in $Ge_{1-x}Sn_x$ alloys, highly doped with As, is still unexplored, further investigation is required in order to deepen the understanding of the defect-donor complexes in As doped $Ge_{1-x}Sn_x$. This analysis reveals that the defect complexes responsible for positron trapping are mono-vacancies. The extensive formation of V-As$_i$ complexes appeared with the increase in the As concentration. We also show that the total As concentration has a significant impact on the formation of the vacancy complexes and the presence of Sn failed to hinder the dopant deactivation.

II. EXPERIMENTAL DETAILS

In this study, we implemented the PAS technique to investigate As doped $Ge_{1-x}Sn_x$ epilayers. A set of six samples was measured. The thicknesses of the $Ge_{1-x}Sn_x$ epilayers were $84 - 88$ nm. The epilayers were grown at 315°C on top of a 600 nm Ge template (referred as Ge-virtual substrates (Ge-VS)) on Si (001) substrates using GeH_4, $SnCl_4$ and AsH_3 as gas precursors in an industrial standard 300 mm RP-CVD tool (Intrepid XP^{TM}). The Ge-VSs were made on regular 300 mm Si wafers using a single step Ge growth, followed by a post-epi anneal at 850C. [26, 27] The samples had threading dislocation densities (TDD) of $\sim 3 - 6 \times 10^7$ cm^{-2} as extracted from defect etching and confirmed by electron channeling contrast imaging (ECCI). [28, 29] The growth conditions were kept identical except the partial pressure of AsH_3, which was tuned to reach different As-doping levels in $Ge_{1-x}Sn_x$ layers. The associated material properties of the samples considered in this study are listed in Table I. The total Sn percentage in as-grown $Ge_{1-x}Sn_x$ layers was measured using Rutherford backscattering spectrometry (RBS) and the active carrier concentrations were extracted using Micro-Hall effect (MHE) measurements. A Hall scattering factor (HSF) of 1 has been assumed in this study. The total As concentrations, measured by means of Secondary Ion Mass Spectrometry (SIMS) are shown in Fig. 1. Arsenic quantification was done using Ge standards as GeSn standards for SIMS are not available at the moment. The absolute As level in $Ge_{1-x}Sn_x$ can be slightly off due to difference in sputter- and ion-yield in

$Ge_{1-x}Sn_x$ layers compared to Ge. However, all samples have similar Sn% and a comparison of As levels is therefore still meaningful.

Figure 1. Total As concentration obtained by SIMS for the studied set of samples. The concentration values in the shaded region cannot be trusted, since the sputtering yield of the SIMS measurement is not stable close to the sample surface.

In the PAS technique, we use ^{22}Na which emits positrons. Fast positrons are slowed down and electrostatically accelerated to form a variable energy beam. Once the positrons penetrate the sample, they rapidly loose their energy, then live up to a few hundred pico-seconds in thermal equilibrium with the lattice and eventually annihilate with an electron. For a monoenergetic positron beam, the average implantation depth is ~ 10 nm $- \sim 3$ μm, depending on positron energy. Annihilation of positrons with electrons, either in a delocalized state in the lattice or trapped in a defect results in the emission of two γ-quanta with energies of 511 keV. In this process the energy and momentum are conserved. Due to the momentum conservation, the total momentum of the annihilated electron-positron pair is transferred to the annihilation γ-quanta, leading to a Doppler broadening of the annihilation line. The shape of the 511 keV annihilation line is related to the longitudinal momentum distribution of the annihilating electron-positron pair. The open volume defects can be investigated from the momentum distribution obtained from the the annihilation line. A detailed explanation of the PAS technique is discussed in Ref. [16, 17].

Experiments with Doppler broadening spectroscopy (DOBS), referred to as normal-Doppler, were conducted using a high purity Ge detector (HPGe) with a resolution of 1.3 keV at 511 keV. We collected $\sim 10^6$ annihilation events per spectrum in a normal-Doppler experiment. The energies of the mono-energetic positrons were varied from 0.5 to 25 keV. Two shape parameters, conventionally designated as the S- and W- parameters were used to characterize the spectra. The low momentum parameter S, which is also called the valence annihilation parameter, is the fraction of counts in the central region of the annihilation line. On the other hand, the high momentum parameter W, also known as core annihilation parameter, is the fraction of the counts in the wing region of the annihilation line. [16]

We set the S integration energy window as $|p| < 0.46$ a.u., whereas the W integration window was 1.6 a.u. $< |p| < 3.9$ a.u. Here, p denotes the longitudinal Doppler shift in terms of momentum and a.u. signifies the atomic units. An increase (decrease) in the S (W)

Table I. Properties of the studied set of samples. At a mass flow ratio of 1.2×10^{-3} the growth ceases, and no As is incorporated.

[Sn] (%)	Mass flow ratio [AsH$_3$/GeH$_4$]	Active [As]$_{ac}$ (cm^{-3})	Total [As] (cm^{-3})
6.0	5.0×10^{-5}	$3.1(\pm 0.4) \times 10^{19}$	8.3×10^{19}
5.9	1.0×10^{-4}	$5.7(\pm 0.6) \times 10^{19}$	1.6×10^{20}
5.9	3.0×10^{-4}	$8.6(\pm 0.9) \times 10^{19}$	2.5×10^{20}
6.2	1.5×10^{-4}	$7.5(\pm 0.9) \times 10^{19}$	2.6×10^{20}
6.4	6.0×10^{-4}	$5.4(\pm 0.6) \times 10^{19}$	4.4×10^{20}
5.9	4.5×10^{-4}	$5.9(\pm 0.7) \times 10^{19}$	7.4×10^{20}

parameter compared to a defect free reference usually indicates the existence of vacancy defects. The measured annihilation parameters S and W are superpositions of the different annihilation states in the lattice. [16]

$$S = \eta_B S_B + \sum_i \eta_{Di} S_{Di} \tag{1}$$

$$W = \eta_B W_B + \sum_i \eta_{Di} W_{Di} \tag{2}$$

Here, η_B is the fraction of positrons annihilating in the bulk state, and η_{Di} is the fraction of positrons annihilating in the defect state i. S_B (W_B) and S_{Di} (W_{Di}) are the bulk and defect parameters, respectively. If a sample contains only two annihilation states, the $W(S)$-plot of the measurement forms a segment of a line between these states, *e.g.*, bulk and defect states. A deviation from the line between the defect and bulk state indicates that positrons annihilate in more than two annihilation states.

2D-coincidence Doppler broadening spectroscopy (CDOBS), referred to as coincidence-Doppler is an efficient technique to identify vacancy defects and the chemical surroundings of vacancies in the case of vacancy-complexes. After completion of normal-Doppler experiments, coincidence-Doppler measurements were done in order to deepen the understanding of the structure of the vacancy defects. Two HPGe detectors were adopted to detect the Doppler broadening of the 511 KeV annihilation line, in order to measure the momentum intensity of the annihilating electron-positron pairs. The trapping of positrons to vacancies leads to a narrowing of the annihilation peak. The more vacancies in the lattice, the

lower the contribution from core electrons. This results in a reduction of intensity in the high-momentum region of the annihilation line, due to the missing contribution from the absent core electrons. The resolution of the HPGe detector system in the coincidence set-up was 1.0 keV at 511 keV. A positron implantation energy of 4.5 keV was used to maximize annihilation in the epilayer for the CDOBS measurements. Approx. 12×10^6 counts for a single spectrum were collected in this experiment. A p-type positron trap free Ge bulk reference sample was used for normalization of the data.

III. RESULTS

Figure 2 shows the W parameters as a function of positron implantation energy for a representative set of samples. The average positron implantation depth calculated for Ge is shown on the top axis. At the positron implantation energies of $3.5-6$ keV, the contribution to the annihilation comes predominantly from the epilayer. Shorter e^+ diffusion lengths yield steeper slopes in the energy interval $0-4$ keV. The samples with higher total As concentration contain higher vacancy concentrations, which results in shorter diffusion lengths and a visible plateau in the W parameter in the energy interval $3.5-6$ keV, since positrons are getting trapped in the vacancies in the epilayer. The epitaxial layer in the $Ge_{0.94}Sn_{0.06}$ sample, with total As concentration of 8.3×10^{19} cm^{-3} (marked with open black circles), is challenging to trace out in the energy interval $3.5-6$ keV due to the longer e^+ diffusion length. This indicates a lower e^+ trap concentration due to lower defect concentration in the samples with lower total As concentration. The $Ge_{0.94}Sn_{0.06}$ sample shows a higher W parameter value of ~ 0.036, at the energies of $0-2$ keV compared to the other two samples shown in Fig. 2. A similar surface behaviour was observed for the $Ge_{0.94}Sn_{0.059}$ sample grown with a total As concentration of 1.6×10^{20} cm^{-3} (Table I).

Figure 2. *W(E)* plots for samples with different total As concentrations. The error in the W parameter is approx. ± 0.0001. The top axis presents the average positron implantation depth calculated for Ge.

Figure 3 presents the W parameter as a function of the S parameter for the same samples as in Fig. 2. The e^+ annihilation states at the surface, in the epitaxial layer, in the Ge-VS and in the substrate are indicated for samples with different total As concentration.

However, no clear state in the epilayer is noticeable for the $Ge_{0.94}Sn_{0.06}$ sample epilayer with total As concentration of 8.3×10^{19} cm^{-3}. The surface state in the $Ge_{0.94}Sn_{0.06}$ sample is different from the other two samples in Fig. 3.

Figure 3. The *W (S)* plot for three samples with different total As concentrations. Lines to guide the eyes are drawn for the better understanding of the e$^+$ trapping in the epilayers. The arrows indicate the increasing e$^+$ implantation energy. The errors for the S and W parameters are approx. ± 0.0005 and ± 0.0001, respectively. Surface, epilayer, Ge-Vs, and substrate states are marked with different shapes.

Figure 4 shows the ratio of annihilation line intensities scaled to a p-type defect free Ge reference for samples with different total As concentrations obtained from CDOBS measurements. Two ratio curves from prior studies are shown [22, 23] Kujala *et al.* found mono-vacancy complexes V-As$_i$ in bulk Ge. [22] Kalliovaara *et al.* observed divacancy complexes V$_2$-As$_i$ in highly As doped Ge. [23] The present $Ge_{1-x}Sn_x$:As epilayers resemble the V-As$_i$ behaviour shown by Kujala *et al.* (Fig. 4). [22] The corresponding ratio curves, for experiments done by Kujala *et al.* and for this study exihibit a peak at ~ 1.2 a.u. When the positron wave function is localized in a mono-vacancy, the overlap of the positron wave function with the anisotropic electron momentum distribution in the diamond structure is reduced, which causes the peak at ~ 1.2 a.u. [30] With the increasing size of the open volume in the vacancy defects (*e.g.* V$_2$), the contribution from core electrons in the lattice decreases while the contribution from valence electrons increases. This results in the increase of the S parameter value and hence in the diminishing of the peak at ~ 1.2 a.u., as documented by Kalliovaara *et al.* [23] From the result presented above, we conclude that the corresponding positron traps in the $Ge_{1-x}Sn_x$:As epilayers are mono-vacancy size defects.

Figure 4. Intensity ratio for three different samples with CDOBS. The data were normalized to the data from a p-type defect free Ge sample. Two ratio curves from earlier studies are presented for comparison. V-As$_i$ was included from Ref. [22], whereas, V$_2$-As$_i$ was included from Ref. [23]. The S- and the W-parameter windows are indicated with the shaded regions.

Intensities at high momenta, 1.6 a.u. $< |p| <$ 3.9 a.u. correspond to positrons annihilating mostly with core electrons. The electronic configuration of Ge is $[Ar]3d^{10}4s^24p^2$, while the

8

electronic structure of As is $[Ar]3d^{10}4s^{2}4p^{3}$. The largest contribution in the high-momentum region comes from the $3d$ electron shells. A vacancy forms when an atom from the lattice is missing. The decreased intensity in the high-momentum region for the $Ge_{1-x}Sn_x$:As samples relates to the reduced overlap of the positron wave function with the $3d$ electrons. Due to the similar electronic configuration of Ge and As, the spectra are indistinguishable from each other in the high momentum region.

IV. DISCUSSION

Ge, as well as Si, has the diamond lattice structure, i.e., each Ge atom in the lattice has four nearest neighbours. During growth, vacancies can be abundantly formed in the lattice. These vacancies are mobile [19] until trapped by an impurity atom, in the case of n-type doping by a group V atom. Brotzmann *et al.* suggested that, a doubly negatively charged vacancy forms a defect complex with a positively charged As atom. [14] They reported on the existence of neutral vacancy-donor complexes $(V-As_2)^0$ under extrinsic doping, since the diffusion of n-type dopants is strongly enhanced due to the mobility of the singly negatively charged dopant-vacancy pair $(V-As)^-$. Ranki *et al.* [31] observed the formation of immobile $V-As_3$ complexes from mobile $(V-As)^-$ pairs and $V-As_2$ complexes through the so-called ring mechanism [32] after electron irradiation of highly As doped Si. In a similar fashion, Kujala *et al.* observed $V-As_3$ complexes in Czochralski-grown bulk Ge after in-diffusion of As at 680 °C. [22]

In epitaxial CVD growth, the $V-As_i$ complexes can form directly as well as through diffusion. Hence, in addition to V-As, $V-As_2$ and $V-As_3$, $V-As_4$ complexes can also be formed. With a dopant concentrations of $10^{19} - 10^{21}$ cm^{-3} in the $Ge_{1-x}Sn_x$:As layers, the estimated vacancy concentration is also of the order of $10^{19} - 10^{21}$ cm^{-3}. Increasing the amount of As in the epitaxial growth process, increases the probability of a higher number of As atoms in the mono-vacancy complexes.

Sn belongs to the group-IV elements in the Periodic table and is therefore not electrically active as are the group-V atoms. The Sn atom is also somewhat larger in size than the As atom. In our present samples, there are both a high concentration of As ($10^{19} - 10^{21}$ cm^{-3}), and a high concentration ($\sim 6.0\%$) of Sn. With the high Sn concentration in the Ge lattice, the probability of a Sn atom next to the $V-As_i$ complex is considerable. In

addition, we also documented that in a pure V-Sn complex, the Sn atom relaxes towards the vacancy, creating a split vacancy configuration. [25] Furthermore, according to calculations, this V-Sn complex does not trap positrons, due to the reduction in open volume as the Sn atom relaxes inward [25]. It should also be noted that although these calculations indicate that the stability of the V-Sn$_j$ complex increases slightly with an increasing number of Sn atoms next to the vacancy, the group-V dopant complexes V-D$_i$, where D={P, As, Sb} are energetically favored over V-D$_i$-Sn$_j$ and V-Sn$_j$ in an analogous configuration. However, from a PAS perspective different V-P$_i$ complexes are easier to distinguish from each other, since the electronic configuration of P differs significantly from Ge (outermost core electrons $2p$ in P and $3d$ in Ge) and the atom itself is smaller in size than the lattice atoms Ge and Sn. It is evident from the high momentum region in Fig. 4 that, the intensities for the different samples are very similar in the $p > 2.0$ a.u. This is expected, since the core electronic configuration of As is similar to Ge.

Figure 5. Active As concentrations and W parameters in the sample epilayers as a function of the total As concentration. The average W parameters have been calculated from the energy interval $3.5 - 5$ keV, where the positron localization to the mono-vacancy defects were at a maximum (Fig. 2). The error bars of W parameters are ± 0.0001. A line to guide the eyes is used both for the Active As concentration and for the W parameter.

Figure 5 shows the average W parameter and active As concentration as a function of the total As concentration in the epitaxial Ge$_{1-x}$Sn$_x$ layers. A decreasing trend in the W parameter is seen. The W parameter starts to saturate at the total As concentration of 3.5×10^{20} cm^{-3}. With an increasing amount of As in the growth process, the vacancies created in the growth have more As available to be bound to the vacancy. Hence, at lower total As concentration, the positrons are trapped by a distribution of different V-As$_i$ complexes, these complexes could also contain Sn atoms. However, when the total As concentration is increased, the positrons annihilate in complexes with a higher number of As dopants. When the W-parameter saturates also the number of As atoms in the dominating positron trap reaches a maximum, i.e., V-As$_4$ complexes dominate the positron annihilation. It should be noted that due to the very high dopant concentration, the concentration of vacancies is above the positron saturation trapping limit, i.e., all positrons annihilate in the vacancy complexes. Hence, the PAS technique loses its sensitivity for the defect concentration when

the defect concentration is above $\sim 5 \times 10^{18}$ cm^{-3}. [16]

As the W parameter starts to saturate in Fig. 5, the concentration of active As dopants starts to decrease. Previous studies have shown [23–25] that vacancy complexes are the main compensating defects in highly n-type Ge. Hence, we conclude that with both a high vacancy concentration and a high amount of As atoms available close to the surface during the growth, the vacancies at higher total As concentration trap more dopants. Eventually the V-As$_4$ complex starts to dominate both the trapping of positrons and the compensation of As dopants. Therefore the concentration of active As dopants starts to decrease above a total As concentration of approximately 3.5×10^{20} cm^{-3}. The trend in Fig. 5 was not observed in our previous study of Ge$_{1-x}$Sn$_x$:P. [25] This further strengthens the claim that the binding energy of the vacancy to the dopant increases with an increase in the size of the dopant. [14, 25] Furthermore, the presence of Sn fails to thwart the dopant deactivation, as was observed for P doping in Ref. [25]. Reaching carrier concentrations above 10^{20} cm^{-3} is still a challenge from a production point of view using this growth technique. A possible solution to achieve such high active dopant concentrations could be co-doping of Ge$_{1-x}$Sn$_x$ epilayers with, $e.g.$, P and As, where one of the dopants would be energetically favored to form complexes with the vacancies and the other dopant could contribute to the conductivity.

V. SUMMARY

In conclusion, Doppler broadening and coincidence Doppler broadening spectroscopy were applied to examine vacancy defects in As doped Ge$_{1-x}$Sn$_x$ epilayers. The findings from this research suggest that, mono-vacancy complexes V-As$_i$ are responsible for the passivation of dopants in the highly As doped Ge$_{1-x}$Sn$_x$ samples. The total As concentration and hence the amount of As atoms at the sample surface during growth shows a significant impact on the dominating vacancy defect. Furthermore, the analysis also suggests that the presence of Sn fails to enhance the donor activation.

VI. DATA AVAILABILITY STATEMENT

The data that support the findings of this study are available from the corresponding author upon reasonable request.

[1] E. Haller, Mater. Sci. Semicond. Process. **9**, 408 (2006).

[2] C. Claeys and E. Simoen, *Germanium-based Technologies: From materials to devices* (Elsevier, London, 2011).

[3] K. Brunner, Rep. Prog. Phys. **65**, 27 (2002).

[4] G. He and H. A. Atwater, Phys. Rev. Lett. **79(10)**, 1937-1940 (1997).

[5] R. Loo, B. Vincent, F. Gencarelli, C. Merckling, A. Kumar, G. Eneman, L. Witters, W. Vandervost, M. Caymax, M. Heyns, and A. Thean, ECS J. Solid State Sci. Technol. **2(1)**, N35-N40 (2013).

[6] D. P. Brunco, B. De Jaeger, G. Eneman, J. Mitard, G. Hellings, A. Satta, V. Terzieva, L. Souriau, F. E. Leys, G. Pourtois, M. Houssa, G. Winderickx, E. Vrancken, S. Sioncke, K. Opsomer, G. Nicholas, M. Caymax, A. Stesmans, J. Van Steenbergen, P. Mertens, M. Meuris, and M. M. Heyns, J. Electrochem. Soc. **155(7)**, H552-H561 (2008).

[7] R. C. Ropp, *Solid state chemistry* (Elsevier, Amsterdam, 2003) p. 340.

[8] R. Soref, J. Kouvetakis, J. Tolle, J. Menendez, and V. D'Costa, J. Mater. Res. **22(12)**, 3281-3291 (2007).

[9] X. Gong, G. Han, F. Bai, S. Su, P. Guo, Y. Yang, R. Cheng, D. Zhang, G. Zhang, C. Xue, B. Cheng, J. Pan, Z. Zhang, E. S. Tok, D. Antoniadis, and Y. Yeo, IEEE Electron Device Letters **34(3)**, 339-341 (2013).

[10] R. Milazzo, E. Napolitani, G. Impellizzeri, G. Fisicaro, S. Boninelli, M. Cuscunà, D. De Salvador, M. Mastromatteo, M. Italia, A. La Magna, G. Fortunato, F. Priolo, V. Privitera, and A. Carnera, J. Appl. Phys. **115**, 053501 (2014).

[11] A. Nylandsted Larsen and A. Mesli, Physica B **401**, 85 (2007).

[12] V. Markevich, I. Hawkins, A. Peaker, K. Emtsev, V. Emtsev, V. Litvinov, L. Murin, and L. Dobaczewski, Phy. Rev. B **70**, 235213 (2004).

[13] M. C. Petersen, A. Nylandsted Larsen, and A. Mesli, Phys. Rev. B **82**, 075203 (2010).

[14] S. Brotzmann and H. Bracht, J. Appl. Phys. **103**, 033508 (2008).

[15] S. Brotzmann, H. Bracht, J. Lundsgaard Hansen, A. Nylandsted Larsen, E. Simoen, E. E. Haller, J. S. Christensen, and P. Werner, Phys. Rev. B. **77**, 235207 (2008).

[16] F. Tuomisto and I. Makkonen, Rev. Mod. Phys. **85**, 1583 (2013).

[17] J. Slotte, I. Makkonen, and F. Tuomisto, *Characterisation and control of defects in semiconductors* (The Instituition of Engineering and Technology, London, 2020) pp. 263–284, edited by F. Tuomisto.

[18] A. Polity and F. Rudolf, Phys. Rev. B **59**, 10025 (1999).

[19] J. Slotte, S. Kilpeläinen, F. Tuomisto, J. Räisänen, and A. Nylandsted Larsen, Phys. Rev. B **83**, 235212 (2011).

[20] K. Kuitunen, F. Tuomisto, J. Slotte, and I. Capan, Phys. Rev. B **78**, 033202 (2008).

[21] J. Slotte, M. Rummukainen, F. Tuomisto, V. P. Markevich, A. R. Peaker, C. Jeynes, and R. M. Gwilliam, Phys. Rev. B **78**, 085202 (2008).

[22] J. Kujala, T. Südkamp, J. Slotte, I. Makkonen, F. Tuomisto, and H. Bracht, J. Phys. Condens. Matter **28**, 335801 (2016).

[23] T. Kalliovaara, J. Slotte, I. Makkonen, J. Kujala, F. Tuomisto, R. Milazzo, G. Impellizzeri, G. Fortunato, and E. Napolitani, Appl. Phys. Lett. **109**, 182107 (2016).

[24] A. Vohra, A. Khanam, J. Slotte, I. Makkonen, G. Pourtois, R. Loo, and W. Vandervorst, J. Appl. Phys **125**, 025701 (2019).

[25] A. Vohra, A. Khanam, J. Slotte, I. Makkonen, G. Pourtois, C. Porret, R. Loo, and W. Vandervorst, J. Appl. Phys **125**, 225703 (2019).

[26] V. Terzieva, L. Souriau, M. Caymax, D. Brunco, A. Moussa, S. Van Elshocht, R. Loo, F. Clemente, A. Satta, and M. Meuris, Thin Solid Films **517**, 172 (2008).

[27] G. Wang, R. Loo, E. Simoen, L. Souriau, M. Caymax, M. M. Heyns, and B. Blanpain, Appl. Phys. Lett. **94**, 102115 (2009).

[28] A. Schulze, L. Strakos, T. Vystavel, R. Loo, A. Pacco, N. Collaert, W. Vandervorst, and M. Caymax, Nanoscale **10**, 7058 (2018).

[29] H. Han, T. Hantschel, A. Schulze, L. Strakos, T. Vystavel, R. Loo, B. Kunert, R. Langer, W. Vandervorst, and M. Caymax, Ultramicroscopy **210**, 112922 (2020).

[30] K. Kuitunen, F. Tuomisto, and J. Slotte, Phys. Rev. B **76**, 233202 (2007).

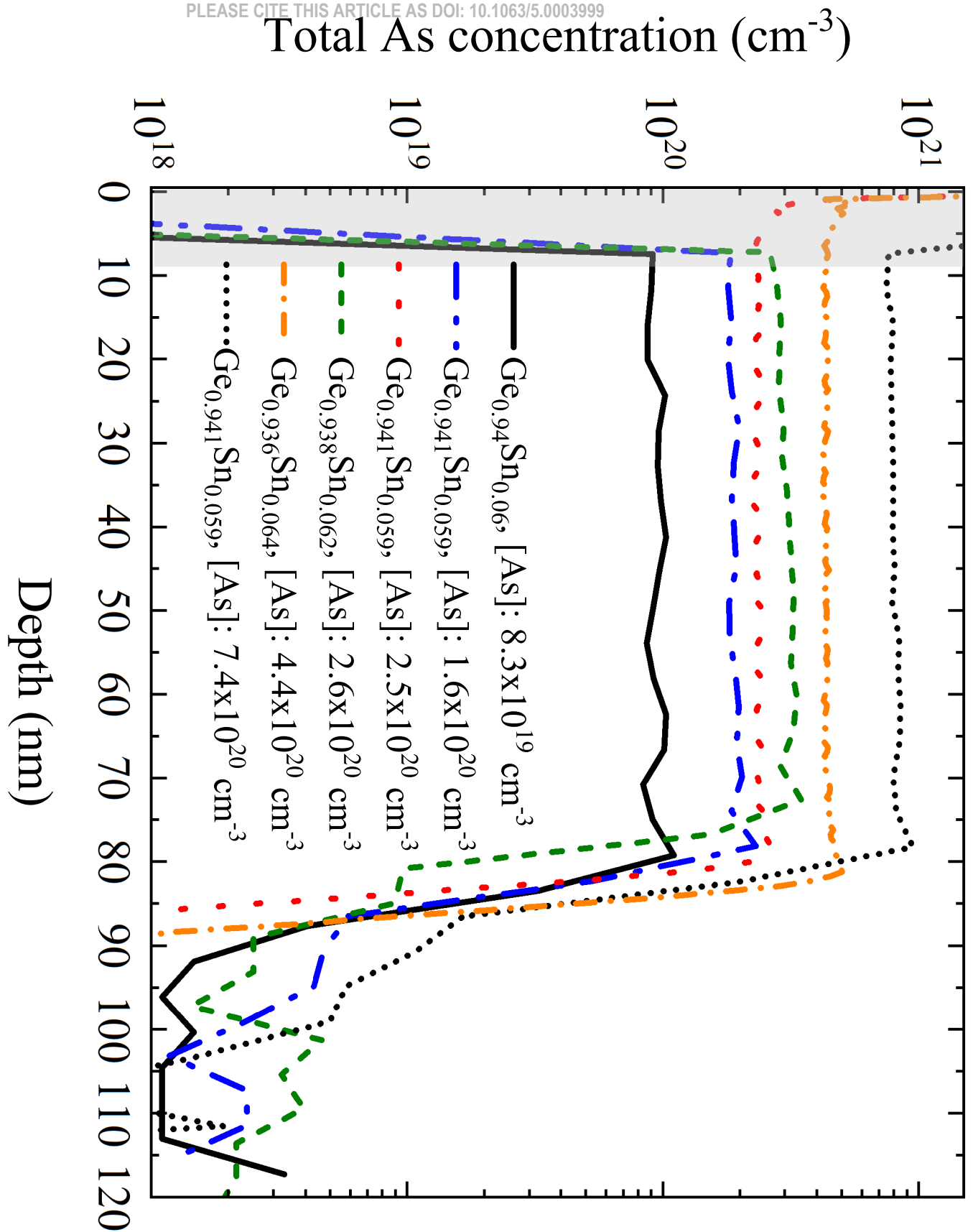[31] V. Ranki, A. Pelli, and K. Saarinen, Phys. Rev. B **69**, 115205 (2004).

[32] M. Ramamoorthy and S. T. Pantelides, Phys. Rev. Lett. **76**, 4753 (1996).

Legend:
- $Ge_{0.94}Sn_{0.06}$, [As]: 8.3×10^{19} cm^{-3}
- $Ge_{0.941}Sn_{0.059}$, [As]: 1.6×10^{20} cm^{-3}
- $Ge_{0.941}Sn_{0.059}$, [As]: 2.5×10^{20} cm^{-3}
- $Ge_{0.938}Sn_{0.062}$, [As]: 2.6×10^{20} cm^{-3}
- $Ge_{0.936}Sn_{0.064}$, [As]: 4.4×10^{20} cm^{-3}
- $Ge_{0.941}Sn_{0.059}$, [As]: 7.4×10^{20} cm^{-3}

Total As concentration (cm^{-3})

Depth (nm)